

University of Nebraska - Lincoln

DigitalCommons@University of Nebraska - Lincoln

---

Anthony F. Starace Publications

Research Papers in Physics and Astronomy

---

January 1997

## Classical interpretation of the quantum description of $H^-$ photodetachment in parallel E and B fields

Qiaoling Wang

*University of Nebraska - Lincoln*

Anthony F. Starace

*University of Nebraska-Lincoln, [astarace1@unl.edu](mailto:astarace1@unl.edu)*

Follow this and additional works at: <https://digitalcommons.unl.edu/physicsstarace>



Part of the [Physics Commons](#)

---

Wang, Qiaoling and Starace, Anthony F., "Classical interpretation of the quantum description of  $H^-$  photodetachment in parallel E and B fields" (1997). *Anthony F. Starace Publications*. 57.  
<https://digitalcommons.unl.edu/physicsstarace/57>

This Article is brought to you for free and open access by the Research Papers in Physics and Astronomy at DigitalCommons@University of Nebraska - Lincoln. It has been accepted for inclusion in Anthony F. Starace Publications by an authorized administrator of DigitalCommons@University of Nebraska - Lincoln.

# Classical interpretation of the quantum description of $H^-$ photodetachment in parallel $E$ and $B$ fields

Qiaoling Wang and Anthony F. Starace

*Department of Physics and Astronomy, The University of Nebraska, Lincoln, Nebraska 68588-0111*

(Received 23 August 1996)

Total quantum mechanical cross sections for photodetachment of  $H^-$  in parallel  $E$  and  $B$  fields are examined both analytically and numerically to extract information which has a classical interpretation, thereby complementing recent classical and semiclassical periodic orbit studies. [S1050-2947(97)09701-1]

PACS number(s): 32.80.Gc

## I. INTRODUCTION

The study of highly excited electrons moving in Coulomb and/or external static electric and magnetic fields has drawn increasing interest from both theorists and experimentalists as a means of exploring the connections between classical and quantum phenomena. One approach is to produce wave packets of electronic states (e.g., by means of short laser pulses) and then examine or modify the nearly classical motion of these packets in real time [1–13]. Another approach is to examine classical or semiclassical electron orbits and then to relate these to features in observed or calculated excitation spectra [14–18]. Still another approach is to carry out measurements using so-called “constant-scaled-energy spectroscopy,” which theoretically permits a link to classical periodic orbits [19,20]. For the case of  $H^-$  photodetachment in parallel external  $E$  and  $B$  fields, two quantum mechanical calculations of the photodetachment cross sections have been carried out [21,22]. However, Peters, Jaffé, and Delos have noted that neither of these two “fully quantum treatments . . . display any connection with classical orbits” [23]. In our own recent quantum mechanical treatment [13], we have made some attempt to make a connection with classical ideas. In this Brief Report we display this connection between our quantum mechanical treatment [13] and classical orbits more precisely.

## II. THEORETICAL BACKGROUND

Full details of our theoretical treatment have been presented elsewhere [13]. Therefore we summarize here only those formulas from Ref. [13] that are required for our analysis presented in the next section. Using an analytic form for the initial state of  $H^-$  having variationally-determined coefficients [24], the photodetachment cross section for  $H^-$  in parallel static electric and magnetic fields may be written analytically as an incoherent sum over partial cross sections  $\sigma_n$  corresponding to the various Landau levels  $n$  describing the electron’s energy of motion in the direction perpendicular to the direction  $\hat{z}$  of the static fields. The result is [25]

$$\sigma = \sum_{n=0}^{\infty} \sigma_n, \tag{1}$$

where

$$\sigma_n = \frac{8\pi^3 b^2 \omega_c}{c \omega^3} \left( \frac{4}{E_S} \right)^{1/3} \left[ \frac{E_S}{\omega} \text{Ai}(-\xi_n) + (2E_S)^{1/3} \text{Ai}'(-\xi_n) \right]^2. \tag{2}$$

In Eq. (2),  $\omega$  is the photon frequency,  $E_S$  is the static electric field,  $\omega_c \equiv B/c$ ,  $b$  is a variationally-determined parameter [24] describing the initial state ( $b=0.315\,52$  a.u.), and the argument of the Airy function and its derivative is given by

$$\xi_n \equiv (2/E_S^2)^{1/3} [\epsilon_i + \omega - \omega_c(n+1/2)]. \tag{3}$$

In Eq. (3),  $\epsilon_i$  is the variationally-determined energy [24] for the initial state ( $\epsilon_i \equiv -0.027\,751$  a.u.). Note that the energy in brackets in Eq. (3) is the electron’s kinetic energy along the  $z$  axis, being equal to the total available kinetic energy ( $\epsilon_i + \omega$ ) less the  $n$ th Landau level energy  $[(n+1/2)\omega_c]$ .

The influence of the parallel  $E$  and  $B$  fields on the  $H^-$  photodetachment cross section near threshold may be demonstrated most clearly by calculation of a modulation factor  $H(E_S, B)$ , which multiplies the field-free detachment cross section for  $H^-$ ,  $\sigma_0$ ,

$$\sigma = H(E_S, B) \sigma_0. \tag{4}$$

Near threshold, the field-free cross section is [26]

$$\sigma_0 = \left( \frac{8\pi^3 b^2}{c \omega^3} \right) \left( \frac{8^{1/2}}{3\pi} \right) (\omega + \epsilon_i)^{3/2}, \tag{5}$$

which clearly shows the Wigner threshold law behavior [27]. Combining Eqs. (1) and (4), we may define also a partial modulation factor  $H_n(E_S, B)$ , as follows:

$$H = \sum_{n=0}^{\infty} H_n \equiv \sum_{n=0}^{\infty} \sigma_n / \sigma_0, \tag{6}$$

where

$$H_n = \frac{3}{2} \omega_c \left( \frac{\pi}{2^{1/2}} \right) \left( \frac{4}{E_S} \right)^{1/3} (\omega + \epsilon_i)^{-3/2} \times \left[ \frac{E_S}{\omega} \text{Ai}(-\xi_n) + (2E_S)^{1/3} \text{Ai}'(-\xi_n) \right]^2. \tag{7}$$

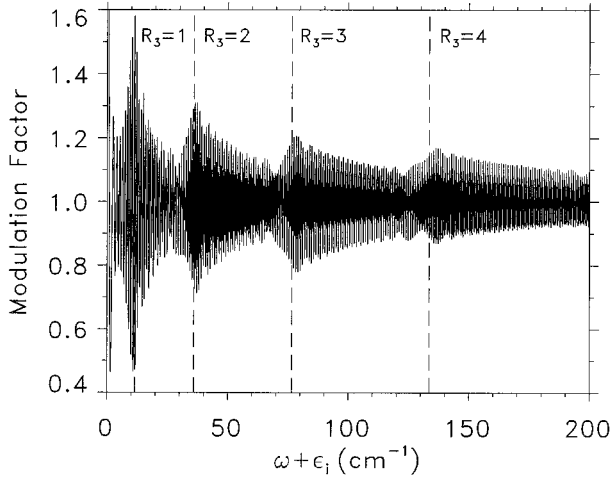


FIG. 1. Modulation factor  $H(E_S, B)$  [cf. Eq. (4)] for the total photodetachment cross section of  $H^-$  in parallel  $E(E_S=60 \text{ V/cm})$  and  $B(B=1 \text{ T})$  static fields plotted vs the energy  $(\omega + \epsilon_i)$  above the zero-field ionization threshold. The dashed lines indicate the energy locations of integer values of the ratio  $R_3 \equiv T_E(n=3)/T_B$  [cf. Eqs. (8) and (9)]. See text for further discussion.

### III. CLASSICAL INTERPRETATION OF THE QUANTUM CROSS SECTIONS

The total modulation factor  $H(E_S, B)$  shown in Fig. 1 clearly demonstrates cross section revivals near  $11 \text{ cm}^{-1}$ ,  $37 \text{ cm}^{-1}$ ,  $77 \text{ cm}^{-1}$ , and  $135 \text{ cm}^{-1}$  for the case  $E_S=60 \text{ V/cm}$  and  $B=1 \text{ T}$ . In Ref. [13] it was noted that these revivals are correlated with integer values of the ratio  $T_E/T_B$ , where  $T_E$  and  $T_B$  are the classical reflection times for electron motion in the static electric and magnetic fields, respectively. The former (describing the electron's motion along the  $z$  axis from the origin to the classical turning point and back) is

given according to Newtonian mechanics by

$$T_E(n) \equiv (2/E_S)[2(\omega + \epsilon_i - \epsilon_{\perp}^n)]^{1/2}, \quad (8)$$

where in our problem the energy for motion perpendicular to the fields is  $\epsilon_{\perp}^n \equiv \omega_c(n+1/2)$ . (Note that for  $B=1 \text{ T}$ ,  $\omega_c=0.934 \text{ cm}^{-1}$  or  $116 \text{ meV}$  so that  $T_E$  has only a weak dependence on  $n$ .) The latter is given by

$$T_B \equiv 2\pi/\omega_c, \quad (9)$$

which is the cyclotron period for the electron. The vertical dashed lines in Fig. 1 show integer values of the ratio  $R_3 \equiv T_E(n=3)/T_B$ , where the choice  $n=3$  was made to give the best overall fit (over the energy range shown) to the calculated revival peaks in the modulation factor. Other than noting that the energies at which revival peaks in the cross section occur are associated with integer values of  $T_E/T_B$ , Ref. [13] omitted any demonstration of how this association follows from the quantum mechanical results. We present two such demonstrations here. In Sec. III A we examine the moiré patterns created by the superposition of the partial cross sections using the analytic formula in Eq. (7). In Sec. III B, we examine the Fourier transform of the numerical results in Fig. 1.

#### A. Moiré effects

The partial modulation factors  $H_n$  are shown in Fig. 2 for even values of  $n$  for  $0 \leq n \leq 16$ . (Note that the odd integer  $H_n$  look very similar, but are not shown in order to conserve space.) Clearly these partial  $H_n$ 's have monotonically decreasing envelopes, with no hint of any broad maxima. Such broad maxima appear only when the  $H_n$ 's are summed. We do so in Fig. 3, where the partial sums

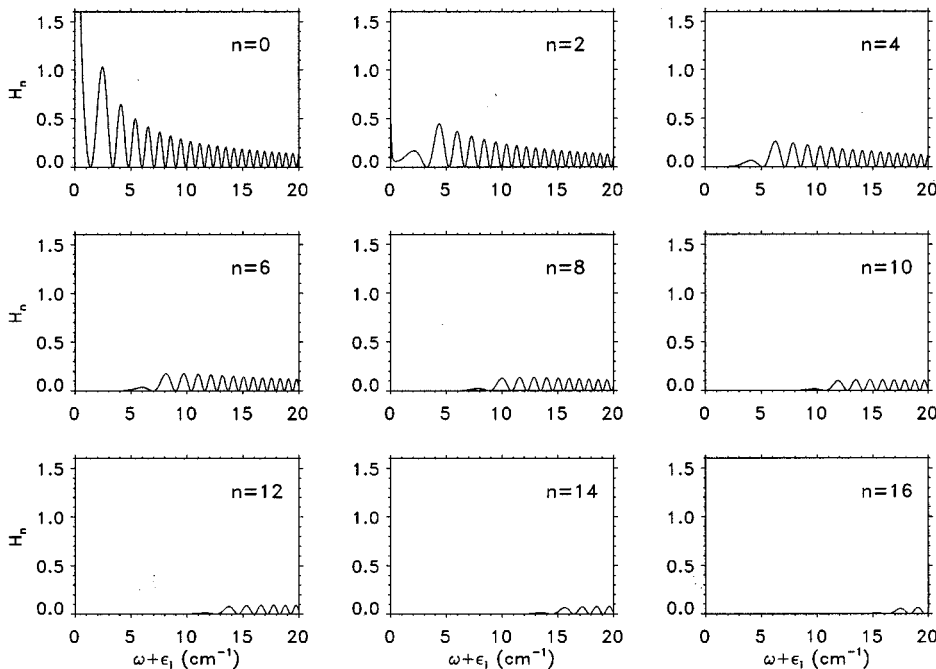


FIG. 2. Partial modulation factors  $H_n$  [cf. Eqs. (6) and (7)] for photodetachment of  $H^-$  in parallel  $E(E_S=60 \text{ V/cm})$  and  $B(B=1 \text{ T})$  static fields plotted vs the energy  $(\omega + \epsilon_i)$  above the zero-field ionization threshold. Only even values of the Landau level  $n$  are shown for  $0 \leq n \leq 16$ ;  $H_n$  for odd  $n$  behave similarly.

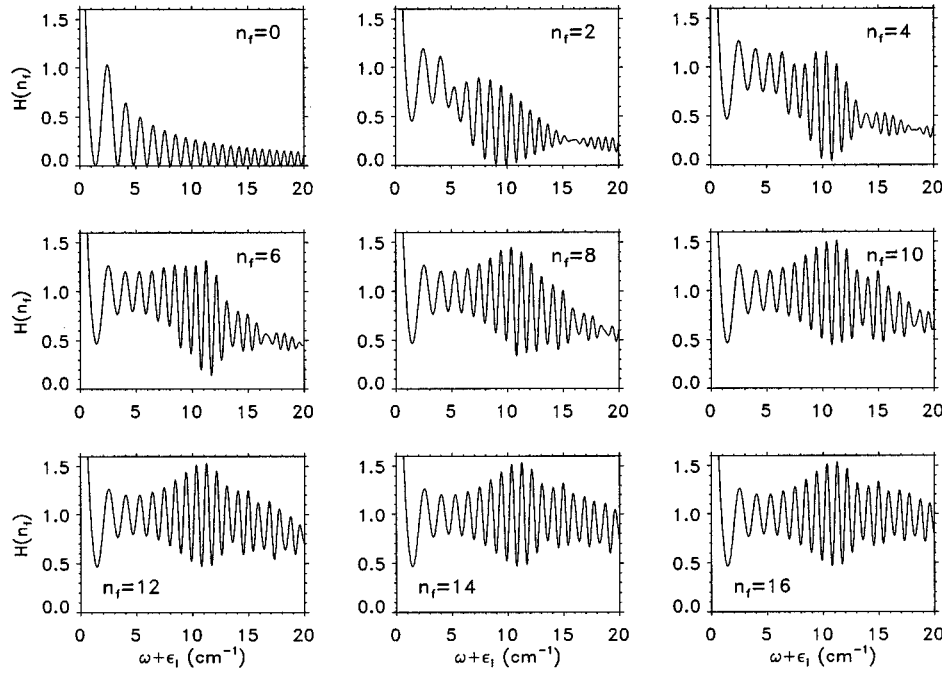


FIG. 3. Plot of the partial summations  $H(n_f) \equiv \sum_{n=0}^{n_f} H_n$  for even values of  $n_f$  over the range  $0 \leq n \leq 16$ . The individual  $H_n$  for even values of  $n$  are shown in Fig. 2. In the limit of large  $n_f$ ,  $H(n_f \rightarrow \infty) \rightarrow H$ , where  $H$  is given in Fig. 1.

$$H(n_f) \equiv \sum_{n=0}^{n_f} H_n \quad (10)$$

are presented for even values of  $n_f$  up to 16. Note that for clarity we have plotted the results only over the energy range from threshold to  $20 \text{ cm}^{-1}$  above. In this energy range the formation of the first cross section revival in Fig. 1 may be observed to stabilize in shape by about  $n_f = 10$ .

This moiré effect in the *incoherent* sum of partial cross sections [Eq. (2)] or modulation factors [Eq. (7)] may be demonstrated analytically to occur at integer ratios of  $T_E/T_B$ . Note first that for typical laboratory electric fields,  $E_S$  is a very small number in atomic units. Hence the arguments  $\xi_n$  [Eq. (3)] of the Airy function and its derivative are large, allowing one to replace them by their asymptotic forms [28]

$$\text{Ai}(-\xi_n) \xrightarrow{\xi_n \rightarrow \infty} \pi^{-1/2} \xi_n^{-1/4} \sin\left(\frac{2}{3} \xi_n^{3/2} + \pi/4\right) \quad (11)$$

$$\text{Ai}'(-\xi_n) \xrightarrow{\xi_n \rightarrow \infty} -\pi^{-1/2} \xi_n^{1/4} \cos\left(\frac{2}{3} \xi_n^{3/2} + \pi/4\right). \quad (12)$$

Clearly the Airy function may be dropped compared to its derivative in Eqs. (2) and (7). Thus, Eq. (7) becomes

$$H_n \xrightarrow{E_S \rightarrow 0} 3\omega_c \frac{[\epsilon_i + \omega - \omega_c(n+1/2)]^{1/2}}{(\epsilon_i + \omega)^{3/2}} \cos^2\left(\frac{2}{3} \xi_n^{3/2} + \pi/4\right). \quad (13)$$

In order to have a moiré effect, the phases of neighboring squared cosine terms must differ by an integer multiple of  $\pi$ , i.e.,

$$\frac{2}{3}(\xi_{n+1}^{3/2} - \xi_n^{3/2}) = \pm \nu\pi, \quad (14)$$

where  $\nu$  is a positive integer. Approximating the difference in the parentheses in Eq. (14) by the derivative of  $\xi_n^{3/2}$  with respect to  $n$ , we obtain

$$\frac{2}{3} \frac{\partial}{\partial n} (\xi_n^{3/2}) = \xi_n^{1/2} (-\omega_c) \left(\frac{2}{E_S^2}\right)^{1/3} = -\nu\pi. \quad (15)$$

Dividing both sides of Eq. (15) by  $-\pi$  and using Eqs. (8) and (9), we find

$$T_E(n)/T_B = \nu, \quad (16)$$

which is the classical relation we sought to deduce from our quantum mechanical formulas. This relation indicates that the revivals in the cross section are associated with classical periodic orbit recurrences at the origin in which the recurrence time for motion in the electric field is a multiple of the recurrence time for motion in the magnetic field.

## B. Fourier transform spectrum

The ratio of electric and magnetic field periods obtained in Eq. (16) is still not quite classical since  $T_E$  depends (albeit weakly) on the Landau quantum number  $n$  for electron motion in the magnetic field. In order to examine the time relationships more precisely (although numerically) for our system, we have taken the Fourier transform of the spectrum in Fig. 1 over the energy range  $0-200 \text{ cm}^{-1}$ . Such Fourier transformations have been found to be useful for interpreting photoabsorption spectra of hydrogen atoms in both magnetic [29–31] and electric [32] fields. They make particular sense for the photodetachment spectra considered here since the “resonances” in energy are quite broad. Our result is shown in Fig. 4, plotted in units of cyclotron periods  $T_B$ , which may be interpreted classically as recurrences at the origin of periodic electron orbits up and back along the static electric field at various multiples of the period for oscillatory motion perpendicular to the magnetic field.

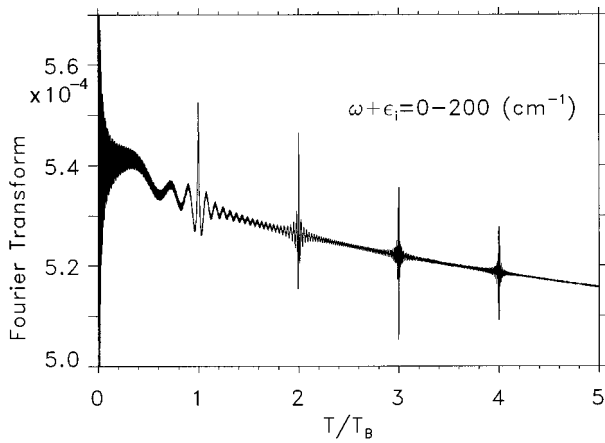


FIG. 4. Fourier transform of the total photodetachment cross section whose modulation factor is presented in Fig. 1. Plotted in units of the cyclotron period  $T_B$  [cf. Eq. (9)].

#### IV. DISCUSSION

In this brief addendum to our earlier work [13], we have examined the quantum mechanical (QM) expressions for photodetachment of  $H^-$  in parallel static  $E$  and  $B$  fields seeking direct evidence for classical periodic orbit behaviors. We

have shown that the QM *partial* cross sections contain no such evidence. Only when the partial cross sections are summed (*incoherently*, of course) does such evidence appear. Analytically one can derive the relation that the revivals of the cross section magnitude correspond to recurrences of classical periodic orbits at the origin by seeking moiré effects among neighboring partial cross sections.

This connection of QM and classical behavior seems rather different from the usual one in which *coherent* sums over QM *amplitudes* are found (in the limit  $\hbar \rightarrow 0$ ) to emphasize paths which follow classical trajectories (owing to the cancellation of amplitudes having different phases except along these trajectories [33–36]). The connection of the Fourier transform spectrum to periodic orbit theory is well-known [29–32]. Our Fourier transform results confirm the moiré effects we deduced. We note finally that in contrast to other works, which seek to determine from periodic orbit or semiclassical studies evidence for features seen in either experiment or results of QM calculations, we have sought in this Brief Report to make some connection to classical periodic orbits directly from the QM results.

#### ACKNOWLEDGMENTS

We thank J. B. Delos for helpful discussions. This work was supported in part by NSF Grant No. PHY-9410850.

- 
- [1] E. J. Heller, *J. Chem. Phys.* **62**, 1544 (1975).  
 [2] W. P. Reinhardt, *J. Phys. B* **16**, L635 (1983).  
 [3] G. Alber, H. Ritsch, and P. Zoller, *Phys. Rev. A* **34**, 1058 (1986).  
 [4] L. D. Noordam, A. ten Wolde, H. G. Muller, A. Lagendijk, and H. B. van Linden van den Heuvel, *J. Phys. B* **21**, L533 (1988).  
 [5] A. ten Wolde, L. D. Noordam, A. Lagendijk, and H. B. van Linden van den Heuvel, *Phys. Rev. Lett.* **61**, 2099 (1988); *Phys. Rev. A* **40**, R485 (1989).  
 [6] L. D. Noordam, A. ten Wolde, A. Lagendijk, and H. B. van Linden van den Heuvel, *Phys. Rev. A* **40**, 6999 (1989).  
 [7] G. Alber and P. Zoller, *Phys. Rep.* **199**, 231 (1991).  
 [8] L. D. Noordam, D. I. Duncan, and T. F. Gallagher, *Phys. Rev. A* **45**, 4734 (1992).  
 [9] B. Broers, J. F. Christian, J. H. Hoogenraad, W. J. van der Zande, H. B. van Linden van den Heuvel, and L. D. Noordam, *Phys. Rev. Lett.* **71**, 344 (1993).  
 [10] Q. Wang and A. F. Starace, *Phys. Rev. A* **48**, R1741 (1993).  
 [11] B. Broers, J. F. Christian, and H. B. van Linden van der Heuvel, *Phys. Rev. A* **49**, 2498 (1994).  
 [12] H. H. Fielding, J. Wals, W. J. van der Zande, and H. B. van Linden van den Heuvel, *Phys. Rev. A* **51**, 611 (1995).  
 [13] Q. Wang and A. F. Starace, *Phys. Rev. A* **51**, 1260 (1995).  
 [14] J. B. Delos, R. L. Waterland, and M. L. Du, *Phys. Rev. A* **37**, 1185 (1988).  
 [15] J.-M. Mao, K. A. Rapelje, S. J. Blodgett-Ford, and J. B. Delos, *Phys. Rev. A* **48**, 2117 (1993).  
 [16] M. A. Iken, F. Borondo, R. M. Benito, and T. Uzer, *Phys. Rev. A* **49**, 2734 (1994).  
 [17] (a) A. D. Peters, C. Jaffé, and J. B. Delos, *Phys. Rev. Lett.* **73**, 2825 (1994); (b) (unpublished).  
 [18] A. D. Peters, C. Jaffé, J. Gao, and J. B. Delos (unpublished).  
 [19] A. Holle, J. Main, G. Wiebusch, H. Rottke, and K. H. Welge, *Phys. Rev. Lett.* **61**, 161 (1988).  
 [20] U. Eichmann, K. Richter, D. Wintgen, and W. Sandner, *Phys. Rev. Lett.* **61**, 2438 (1988).  
 [21] M. L. Du, *Phys. Rev. A* **40**, 1330 (1989).  
 [22] I. I. Fabrikant, *Phys. Rev. A* **43**, 258 (1991).  
 [23] Reference [17(a)]. Cf. comments in their Ref. [3].  
 [24] T. Ohmura and H. Ohmura, *Phys. Rev.* **118**, 154 (1960).  
 [25] Cf. Ref. [13], Eqs. (45) and (46).  
 [26] Bo Gao, Ph.D. thesis, The University of Nebraska–Lincoln, 1989. See Appendix D, Sec. D.1(a), Eq. (D.25).  
 [27] E. P. Wigner, *Phys. Rev.* **73**, 1002 (1948).  
 [28] *Handbook of Mathematical Functions*, edited by M. Abramowitz and I. A. Stegun (Dover, New York, 1964), Eqs. 10.4.60 and 10.4.62.  
 [29] A. Holle, G. Wiebusch, J. Main, B. Hager, H. Rottke, and K. H. Welge, *Phys. Rev. Lett.* **56**, 2594 (1986).  
 [30] J. Main, G. Wiebusch, A. Holle, and K. H. Welge, *Phys. Rev. Lett.* **57**, 2789 (1986).  
 [31] J. Main, G. Wiebusch, K. Welge, J. Shaw, and J. B. Delos, *Phys. Rev. A* **49**, 847 (1994).  
 [32] J. Gao and J. B. Delos, *Phys. Rev. A* **49**, 869 (1994).  
 [33] K. W. Ford and J. A. Wheeler, *Ann. Phys.* **7**, 259 (1959); **7**, 287 (1959).  
 [34] R. P. Feynman and A. R. Hibbs, *Quantum Mechanics and Path Integrals* (McGraw-Hill, New York, 1965).  
 [35] M. V. Berry and K. E. Mount, *Rep. Prog. Phys.* **35**, 315 (1972).  
 [36] W. H. Miller, *Adv. Chem. Phys.* **25**, 69 (1974).